University Library



A gateway to Melbourne's research publications

Minerva Access is the Institutional Repository of The University of Melbourne

Author/s:
Liu, HH;He, Z;Nguyen, CTO;Vingrys, AJ;Bui, BV

Title:
Reversal of functional loss in a rat model of chronic intraocular pressure elevation

Date:
2017-01-01

Citation:
Liu, H. H., He, Z., Nguyen, C. T. O., Vingrys, A. J. & Bui, B. V. (2017). Reversal of functional loss in a rat model of chronic intraocular pressure elevation. Ophthalmic and Physiological Optics, 37 (1), pp.71-81. https://doi.org/10.1111/opo.12331.

Persistent Link:
https://hdl.handle.net/11343/291874

Received Date : 09-Aug-2016

Revised Date : 16-Sep-2016

Accepted Date : 17-Sep-2016

Article type : Original Article

Author Manuscript

Title Page

Full title: Reversal of functional loss in a rat model of chronic intraocular pressure elevation

Running head: Recovery from chronic IOP elevation

Authors' names and institutional affiliation: Hsin-Hua Liu, Zheng He, Christine TO Nguyen, Algis J Vingrys, Bang V Bui

Department of Optometry & Vision Sciences, University of Melbourne, Victoria, Australia

Corresponding author:
Bang V Bui
E-mail address: bvb@unimelb.edu.au

Keywords: intraocular pressure, circumlimbal suture, glaucoma, recovery, electroretinogram, rat, optical coherence tomography

This is the author manuscript accepted for publication and has undergone full peer review but has not been through the copyediting, typesetting, pagination and proofreading process, which may lead to differences between this version and the Version of Record. Please cite this article as doi: 10.1111/opo.12331

This article is protected by copyright. All rights reserved

This article is protected by copyright. All rights reserved

Author Manuscript

Abstract

Purpose: This pilot study considered whether intraocular pressure (IOP) lowering could reverse ganglion cell dysfunction in a rat model of chronic ocular hypertension.

Methods: A circumlimbal suture was applied in one eye to induce ocular hypertension (n = 7) in Long-Evans rats. The contralateral eye served as an untreated control. After eight weeks of IOP elevation the suture was removed to lower IOP for the remaining seven weeks. Electroretinogram (ERG) and optical coherence tomography (OCT) were measured at baseline, 2, 4, 8, 12 and 15 weeks. Retinae were collected for histology at week 15.

Results: In sutured eyes, IOP was elevated by 7 to 11 mmHg above control eyes (12 ± 0.2 mmHg [standard error of the mean]). Eight weeks of chronic IOP elevation resulted in a reduction of the ganglion cell mediated positive Scotopic Threshold Response (pSTR, -25 ± 7% of baseline), as well as smaller photoreceptor (-7 ± 4%) and bipolar cell mediated responses (-6 ± 5%). After suture removal, IOP recovered to normal. By 15 weeks the a-wave (0 ± 6%), b-wave (-2 ± 6%) and pSTR had recovered back to baseline (from -25 ± 7% to -4 ± 6%). The retinal nerve fiber layer was thinned by -9 ± 3% at week 8 and showed no further decline at week 15 (-10 ± 2%). Cell numbers in the ganglion cell layer were similar between suture removal and control eyes at week 15 (3543 ± 478 vs 4057 ± 476 cells/mm^2).

Conclusions: The circumlimbal suture model might be a useful platform to study the reversibility of neuronal dysfunction from chronic IOP challenge.

Author Manuscript

Introduction

It is well known that intraocular pressure (IOP) reduction is the mainstay of glaucoma treatment, helping to halt progression and to prevent further retinal ganglion cell (RGC) loss. However, whether neuronal injury is reversible with IOP lowering remains less certain. Studies in humans[1] and rodents[2] have shown that functional deficits associated with mild transient IOP elevation are reversible, with the rate of recovery dependent on both the magnitude and duration of the insult.[3] As vision loss

This article is protected by copyright. All rights reserved

in glaucoma is thought to be irreversible there must be an IOP-related injury threshold above which RGC injury becomes permanent.

The concept of reversibility of RGC dysfunction has been considered by assaying function before and after therapeutic IOP reduction in human subjects. Studies have shown that reductions in electroretinogram (ERG) amplitude can recover after IOP lowering in patients with ocular hypertension and glaucoma.[4-7] A recent study reported short-term enhancement of visual field sensitivity following IOP reduction.[8] However, not all studies have demonstrated that retinal dysfunction in glaucoma is reversible.[9] One possible reason for the disparity between studies is the timing of intervention. It may be that IOP lowering early in the course of injury facilitates recovery, whereas later intervention only prevents further decline. There is growing evidence that early changes to ganglion cell structure and function precede cell loss.

Studies of chronic IOP elevation suggest that RGC dysfunction can precede thinning of the retinal nerve fibre layer (RNFL), as measured using optical coherence tomography (OCT).[1, 10, 11] Indeed, OCT has been shown to be insensitive to subtle RGC microtubule injury in the earliest stages of chronic IOP injury in non-human primates.[11, 12] Early functional deficits have been attributed to changes in RGC morphology, such as shrinkage of dendritic fields, reduction in dendrite complexity and changes to axonal integrity as has been reported in non-human primate models of glaucoma[11, 13] and mouse models of optic nerve crush.[14, 15] IOP elevation can also directly affect pressure sensitive channels on RGCs and their axons altering membrane potentials and thus their reactivity to light.[16] These studies raise the possibility of an epoch early in the course of IOP elevation, before substantive structural loss, during which RGCs are dysfunctional but retain the capacity to recover with IOP lowering.

We hypothesise that RGC dysfunction consequent to chronic ocular hypertension in rats is reversible provided that IOP-lowering is initiated prior to significant RNFL thinning, as measured using OCT. In a previous study we showed in a rat model of chronic ocular hypertension[10] that eight weeks of IOP elevation produces RGC dysfunction (smaller positive Scotopic Threshold Response [pSTR]) with subtle but insignificant RNFL thinning, which then progressed to RGC dysfunction with robust RNFL thinning and cell loss by 15 weeks. Thus in this model eight weeks provides a

This article is protected by copyright. All rights reserved

Author Manuscript

useful time point to test our hypothesis for the reversibility of IOP dysfunction before the onset of RNFL thinning.

Materials and methods

Animals

All experimental procedures were in compliance with the National Health and Medical Research Council Australian Code of Practice for the care and use of animals for scientific purposes. Animal ethics was approved by the Florey Animal Ethics Committee at the University of Melbourne (Ethics number: 13-044-UM). All animals used in this study were male Long-Evans rats (eight to ten weeks old, 300 ~ 400 g at the start of experiment). They were housed in a 20℃ environment with light cycling (12-hour light/12-hour dark, 50 lux maximum). Food (WEHI, Barastoc, http://www.agriproducts.com.au/) and water were available *ad libitum*.

Fourteen eyes were examined in seven consecutive animals allowing intra-animal comparisons. Each animal had their circumlimbal suture and control treatments randomised between right and left eyes The sutured eye had eight weeks of IOP elevation followed by seven weeks of IOP reduction comprising a total 15 weeks of observation.

IOP elevation, monitoring and lowering

Procedures for IOP monitoring (rebound tonometer) and IOP elevation by circumlimbal suture have been described in detail previously.[10] In brief, rats were acclimatised for a week prior to experimentation. IOP was assayed in awake animals using a rebound tonometer (Tonolab, http://www.icaretonometer.com/) without topical anesthesia, on four consecutive days to establish baseline. Measurements were conducted between 10 am and 12 pm under the same lighting conditions (200 lux at the bench top) to control for diurnal IOP fluctuations.

To raise IOP, animals under isoflurane anesthesia (5% induction and 2% maintenance at 2 L/min) were placed on a heating pad (http://www.soundveterinary.com.au/). For corneal anesthesia, one drop of 0.5% proxymetacaine (https://www.alcon.com/eye-care-products) was applied. A circumlimbal suture (8/0, nylon) was placed around the equator of the eye at a

This article is protected by copyright. All rights reserved

Author Manuscript

distance of approximately 1.5 mm behind the limbus. The suture was anchored by placing it below the conjunctiva, avoiding the major episcleral drainage veins at five to six anchor points evenly spaced around the globe. The anterior position of the suture avoided congestion of the vortex veins. Contralateral eyes served as untreated controls.

IOP readings were taken immediately (two minutes) and at one hour after suture application. For the first week, IOP was measured daily, and for the rest of the experimental period, IOP was measured three times a week. All IOP measurements were conducted without general or topical anesthesia with the exception of the two minute time point, when rats remained under the influence of surgical isoflurane. At the end of week 8, the suture was cut and removed under isoflurane anesthesia (~10 minutes) to lower IOP for the remaining seven weeks of experimentation.

Electroretinography

ERG responses were measured following dark adaptation (12 hours) at baseline, and at weeks 2, 4, 8, 12 and 15 after suture implantation. ERG acquisition and analysis have been described in detail previously.[17-19] In brief, dark-adapted rats had general anesthesia induced (intramuscular ketamine 60 mg/kg and xylazine 5 mg/kg, http://www.troylab.com.au) followed by a drop of 0.5% proxymetacaine and one of 0.5% tropicamide to produce corneal anesthesia and mydriasis, respectively. ERG stimuli were presented starting from -6.35 and progressing up to 2.07 log cd.s.m^{-2} via a calibrated light emitting diode (LED) Ganzfeld sphere (http://www.photometricsolutions.com/). Custom-made chlorided silver electrodes were used to measure responses. The positive electrode was placed on the apex of the cornea and the reference ring-shaped electrode was gently looped near the equator of the eye. A ground needle electrode (http://www.natus.com/) was subcutaneously inserted in the tail. ERG responses were acquired at a sampling rate of 4000 Hz (http://www.adin-struments.com/), with bandpass filters of 0.3 to 1000 Hz (-3dB, pre-amplifier model P511; Grass Technologies, http://www.natus.com/).

To quantify the photoreceptor response, the a-wave (also known as the “P3”) in response to the brightest stimuli (2.07 log cd.s.m^{-2}) was modelled using A delayed-Gaussian function (P3 model) to return the amplitude (Rm_{P3}, or maximum response of the P3, μV) and sensitivity of phototransduction.[20, 21] The bipolar cell response was

This article is protected by copyright. All rights reserved

Author Manuscript

analysed by subtracting the P3 model from the raw ERG waveform to return a more accurate measure of the b-wave (also known as the "P2"). The P2 peak amplitude as a function of luminous energy was then described by fitting a hyperbolic function[22] to return the maximum amplitude (Vmax, μV). RGCs contribute substantially to the pSTR at -5.01 log cd.s.m^2 in rats. The response at -5.01 log cd.s.m^2 was low-pass filtered and the pSTR amplitude was quantified at a fixed time of 110 ms after stimulus onset.

Optical coherence tomography

Following anesthesia, mydriasis and ERG measurement, animals were placed on a platform with circulating heated water to maintain body temperature. A lubricant (GenTeal, https://www.novartis.com.au/) was applied to the eye to maintain corneal moisture and to act as an optical coupling medium to the eyepiece of the OCT system (Micron III, http://www.phoenixreslabs.com/). Imaging was performed at baseline, then at 2, 4, 8, 12 and 15 weeks. A horizontal B-scan (1024 A-scans, 2 μm axial resolution, 1.8 μm lateral resolution and a 50 degree field of view) through the centre of the optic nerve, avoiding any of the major vessels was measured (*Supplementary Figure 1*). Care was taken to scan in similar regions across the weeks. Ten B-scans were averaged for image analysis using ImageJ software (https://www.nih.gov/). A masked observer manually segmented the inner limiting membrane, retinal nerve fibre layer (RNFL) and Bruch's membrane. Average total retinal thickness (from inner limiting membrane or ILM to Bruch's membrane) and RNFL thickness (ILM to RNFL) were taken for regions 200 to 400 μm both temporal and nasal to the center of the optic nerve head (*Supplementary Figure 1*).

Histology

Following ERG and OCT measurement at 15 weeks, animals were terminated by intracardial injection of pentobarbital (0.3 mL, Lethabarb, https://www.virbac.com.au/). Eyes were immediately enucleated and the cornea pierced with a 30 gauge needle to allow fixative (10% neutral buffer formalin) to enter the eye. Prior to paraffin embedding and sectioning, ocular tissues were dehydrated with 70%, 95% and 100% ethanol, treated with chloroform (https://www.sigmaaldrich.com/) and embedded in paraffin blocks. Sections of 10 μm were cut and three consecutive sections containing the full profile of the optic nerve

This article is protected by copyright. All rights reserved

Author Manuscript

head was mounted on glass slides (Superfrost Plus, https://www.thermofisher.com/). Each slide was dewaxed, rehydrated and stained with hematoxylin and eosin (H & E). All slides were scanned with an Aperio ScanScope® CS (http://www.leica.com/) at 20x magnification. Images were analysed in Aperio ImageScope software (Leica). The cell density in the GCL was counted over an area of 250 x 20 μm^2, starting at 200 µm lateral to the scleral canal opening by a masked observer. Cell counts from both sides of the optic nerve were averaged to return a value for that retinal sample. For each eye, cell count data was the average of three consecutive sections.

Statistics

All data are given as mean ± standard error of mean (SEM), except for *Figure 3* where 95% confidence limits are presented with the ERG waveforms. Statistical analysis was conducted using Genstat (https://www.vsni.co.uk/software/genstat/). To compare data between control and treated eyes a linear mixed model (REML) was used which takes into account the two within subject factors, time and control/treated eye [23, 24]. Post-hoc comparison using Bonferroni corrections was used to compare control and treated eyes at the various time points.

Results

The IOP profile following circumlimbal suturing is shown in *Figure 1*. There was an initial IOP spike immediately (two minutes) following suture application of 50 ± 4 mmHg, which by one day was 34 ± 3 mmHg. IOP remained significantly higher than the control eye over the next eight weeks (21.9 ± 0.6 vs 12.5 ± 0.2 mmHg, $F_{1,49}$ = 32.8, $p < 0.001$, linear mixed model analysis). Within a day of suture removal IOP had significantly recovered from 20 ± 0.4 to 14 ± 0.6 mmHg (33 ± 2% reduction, $p < 0.001$, linear mixed model analysis). After suture cut, from week 8 to week 15, IOP remained statistically similar to the fellow control eye (12.9 ± 0.2 vs 11.5 ± 0.3 mmHg $p > 0.05$, linear mixed model analysis).

The effect of chronic IOP elevation and IOP lowering on the ERG is shown in *Figures 2* and *3*. *Figure 2* shows ERG responses for a range of luminous energies, at three key time points. In comparison to baseline (*Figure 2A*) there was a small reduction of amplitude of all ERG components. At week 15 (*Figure 2C*), after IOP lowering, there was recovery of waveforms at all luminous energies. *Figure 3A* shows that between

This article is protected by copyright. All rights reserved

Author Manuscript

weeks 2 and 8, IOP elevation produced a small but stable attenuation in the ERG a-wave (photoreceptoral function) and b-wave (bipolar cell function) compared with the control eyes. Over the same time the ganglion cell pSTR was more affected (*Figure 3B*). After suture removal and IOP lowering, the STR recovered.

Figure 4 summarises the amplitude of photoreceptor (a-wave), bipolar cell (b-wave) and RGC (pSTR) function across the 15 weeks of experimentation. In comparison to controls, treated eyes exhibited a small reduction in all ERG components. At week 8, the a-wave was 93 ± 4% of baseline (*Figure 4B*) and the b-wave was similarly reduced to 94 ± 5% (*Figure 4D*). Linear mixed model analysis confirms that the a-wave (*Figure 4A*, $F_1 = 6.4$, $p = 0.014$) and b-wave amplitudes were reduced (*Figure 4C*, $F_1 = 5.9$, $p = 0.018$). At week 15 the a-wave (100 ± 6%) and b-wave (98 ± 6%) amplitude were similar to baseline.

The pSTR was significantly reduced in high IOP eyes (*Figure 4E*, $F_1 = 14.9$, $p < 0.001$). The pSTR had dropped to 75 ± 7% by week 8 ($p < 0.01$). After suture removal, the pSTR recovered to 87 ± 11% at week 12, and 96 ± 6% at week 15 in these same eyes (both $p > 0.05$, Bonferroni's multiple comparison test).

Figure 5 shows the effect of IOP elevation and its subsequent lowering on retinal and RNFL thickness measured using the OCT. There was a significant difference in total retinal thickness between treated and control eyes (*Figure 5A*, $F_1 = 12.8$, $p < 0.001$ linear mixed model analysis) however post hoc analysis revealed no particular significance at any of the weeks ($p > 0.05$, Bonferroni post-hoc). In contrast, in treated eyes RNFL thickness was reduced from 22.6 ± 0.6 μm at baseline to 20.6 ± 0.7 μm at week 8. After IOP lowering, RNFL thickness did not change significantly at week 12 (20.4 ± 0.7 μm) and week 15 (20.4 ± 0.8 μm) when compared with week 8 (*Figure 5D*). Linear mixed model analysis confirmed the significant time and treatment interaction ($F_{1,5} = 3.7$, $p = 0.005$), with post hoc-analysis (Bonferroni's multiple comparison test) indicating that RNFL was significantly thinner in treated compared with control eyes at weeks 8, 12 and 15 ($p < 0.01$).

After 15 weeks, cell density in the ganglion cell layer (GCL) was assessed with retinal cross sections. In general, there was no gross damage to retinal structure in both groups (*Figure 6A* and *6B*). GCL cell density was not significantly different between

This article is protected by copyright. All rights reserved

Author Manuscript

treated and fellow control eyes (*Figure 6C*, 3543 ± 478 vs 4057 ± 476 cells/mm^2, paired t-test, passed Shapiro-Wilk normality test, $t_6 = 1.3$, $p = 0.26$).

Figure 7 considers the relationship between the various outcomes measured at 15 weeks. *Figure 7A* shows that the correlation between a-wave amplitude and RGC layer cell density was not significant. In contrast, retinae with higher RGC cell density tended to have higher pSTR amplitude (*Figure 7B*, $p < 0.01$, $r^2 = 0.76$). Whilst there was a tendency for eyes showing higher RGC cell density to have thicker RNFL this was not significant (Figure 7C, $p = 0.22$, $r^2 = 0.12$). There was a modest relationship between the pSTR and RNFL thickness (*Figure 7D*, $p = 0.02$, $r^2 = 0.40$).

Discussion

Previously we have shown using the same circumlimbal suture model that 15 weeks of sustained mild ocular hypertension produced inner retinal dysfunction and a reduction in RGC layer cell density.[10] We also showed that there was a progressive thinning of RNFL thickness between weeks 8, 12 and 15. Up until the eighth week the IOP profile, along with the ERG and OCT changes in this study gave similar trends to those previously reported.[10] In this follow up pilot study, we show that IOP lowering after eight weeks of ocular hypertension resulted in recovery of the pSTR. The progressive thinning of the RNFL and the cell loss in the ganglion cell layer found previously between weeks 8 and 15 were not seen in eyes that had IOP restored to normal levels. These data provide preliminary evidence for functional recovery from a prolonged period of IOP elevation. This is consistent with reports of functional recovery in patients treated to lower IOP. These studies demonstrated improvement of visual field sensitivity[8, 25, 26] and ganglion cell mediated components of the ERG following IOP reduction, either by surgical or pharmacological intervention.[4, 5, 7] Similar functional recovery has been noted following acute IOP elevation in human subjects[27] and in laboratory models.[28, 29]

Suture removal provides a simple means for IOP reduction and thus stress removal, free of potential pharmacological confounds. At week 8, IOP was reduced by 33 ± 2%. A previous study showed that IOP reduction of 38% in the DBA/2J mouse glaucoma model was associated with an 83% improvement in the pattern ERG, a robust improvement in RGC function.[30] This is qualitatively consistent with the pSTR recovery seen in this study. The recovery of the pSTR was gradual following IOP

This article is protected by copyright. All rights reserved

Author Manuscript

reduction (*Figures 3B, 4E* and *4F*). Specifically, at week 8, immediately prior to suture removal, the pSTR was reduced to 75 ± 7% relative to baseline. By week 12 and week 15, the pSTR had recovered to 87 ± 11% and 96 ± 6% of baseline, respectively. This prolonged time course may provide a useful window over which to study cellular processes mediating recovery from chronic IOP challenge. Interestingly, outer retinal function (a/b-wave) also appeared to recover at week 15, although they was much less attenuation at week 8 when compared with the pSTR. Although it is possible that improvement in outer retinal function can lead to a larger pSTR,[31] the relative change in the pSTR between weeks 8 and 15 is much greater than would be predicted based on the outer retinal improvement.

The capacity for the pSTR to recover in this model suggests that we have intervened at a stage of chronic IOP elevation during which ganglion cells have not been irreversibly injured. Interestingly, we found that RNFL thinning did not recover (*Figure 5C* and *5D*) even though function had significantly improved (*Figure 4F*), and there was no cell loss (*Figure 6C*). This finding suggests that at eight weeks there may have been structural changes such as synaptic or dendritic changes that are irreversible. At week 15 there was a relationship between RGC layer cell density and pSTR amplitude (*Figure 7B*), whereas the correlation between RNFL thickness and pSTR amplitude was more modest (*Figure 7D*). Given that dysfunction may involve altered synapses and reduced dendritic complexity[14, 32-35] why RNFL thickness did not recover along with the pSTR is unclear. One possibility is that the remain cells increase their output, which might happen due to the beneficial effects of reactive gliosis (or astrogliosis) in maintaining neurons and their synapses. This important role for astrocytes has been demonstrated in the brain during ischemic insult.[36, 37] Studies using more sensitive tools to assess ganglion cell structure and synaptic inputs along with glial cell activation are needed to better understand the relationship between functional recovery and the structural modifications that may underlie these changes.

The cellular mechanisms by which IOP elevation can lead to RGC dysfunction are thought to involve disruption of axonal transport, excess glutamate activation of N-methyl-D-aspartate (NMDA) receptors, impaired glial cell function, vascular and bioenergetics factors, and more recently activation of pressure sensitive channels such as transient receptor potential (TRP) and purinergic receptors have also been implicated.[16, 38-46] With IOP lowering, one or some of these sources of stress on optic

This article is protected by copyright. All rights reserved

Author Manuscript

nerve axons and RGCs may be relieved. One might speculate that the underlying mechanisms should exhibit a similar time course to the recovery of the pSTR, which took between four to seven weeks after IOP lowering. One possibility is that pSTR recovery is associated with gradual resumption of axonal transport and the resupply of neurotrophic factors, as brain derived neurotrophic factor is known to prevent IOP induced retinal dysfunction in laboratory models of glaucoma.[47, 48]

Another possibility is that IOP lowering modifies stretch sensitive channels to improve RGC excitability. Sappington, *et al*.[49] recently reported that TRP vanilloid-1 (TRPV1) and TRPV4 expression increase and decrease, respectively, with higher IOP in the DBA2J mouse model of chronic IOP. Activation of TRPV4 channels found on ganglion cell dendrites is known to increase RGC excitability.[45] Thus restoration of TRPV1 and TRPV4 expression could contribute to recovery of the pSTR seen in this study. Whilst speculative, this mechanism might account for our finding that there is no RNFL recovery, despite near complete pSTR recovery.

Although IOP reduction alleviated RGC dysfunction in this study, it must be noted that these are young animals. A number of studies suggest that the capacity for functional recovery from IOP elevation is reduced with age.[30, 50] Furthermore, the systematic application of the general anaesthetic compound, ketamine, has been reported to have neuroprotective effect in rats through inhibition of tumour necrosis factor-α and interleukin-6.[51] Therefore, this might confound the effect of IOP reduction observed in our study. However, rat eyes that had undergone circumlimbal suture IOP elevation throughout 15 weeks using the same repeated anaesthesia regimen did not show recovery.[10] Thus it is unlikely that repeated ketamine anaesthesia is entirely responsible for the pSTR recovery seen in this study.

The current study has limitations. This is a preliminary study and provides information on only a small cohort of sutured and contralateral control eyes. Although the changes seen here at eight weeks are consistent with those we have previously reported,[10] our sample size returns a statistical power that is lower than is desirable. Power analysis, taking the RGC-derived pSTR as the most relevant component of recovery following IOP reduction (coefficients of variation pSTR 23%) with a sample size of seven give a statistical power of 50%. Ideally, another cohort of animals with IOP elevation throughout the 15 weeks of experimentation would aid comparison. This positive control group would not only provide direct comparison of functional and

This article is protected by copyright. All rights reserved

Author Manuscript

structural changes but also confirm the reproducibility of the suture model, beyond eight weeks. Nevertheless, as the approaches used in this study are identical to those used in our previous study,[10] we fell that comparisons to the eyes that had IOP elevation throughout the 15 weeks is valid. We also acknowledge that the anatomical cell counts employed here while encouraging, provide a limited snapshot of retinal structure and thus require further validation. Finally, although the reference plane use for all OCT imaging was kept constant, no additional correction was made for potential changes in ocular biometric that are associated with the model.

A limitation of the current model is that it has a transient IOP spike immediately after model induction. It is possible that this IOP spike may contribute to some of our ERG and OCT changes. Additionally, the IOP spike could influence the subsequent response of the eye to the chronic component of IOP elevation. Indeed, previous studies have shown that both peak IOP and average magnitude of elevation over time are important determinants of the severity of injury. Previous studies using alternate approaches such as hypertonic saline,[52] episcleral cauterisation[53] laser treatment following intracameral injection of indocyane green[54] have reported IOP peaks (~50 mmHg) similar to those seen here. In those models the a-wave and b-wave showed much greater deficits than the 6 - 7% loss seen in this study (*Figure 4A* and *4B*). Importantly, in the current study it does not appear that the IOP spike has significant long-term effects. If the IOP spike alone were responsible for our functional losses (*Figure 4*) then one would expect that IOP lowering at eight weeks, well after the spike, would not result in recovery of function. That we saw nearly complete recovery of the pSTR (*Figure 4F*) suggests that the chronic IOP component rather than the spike underlies the functional changes seen in this rat model of IOP elevation. Nevertheless, it is important to acknowledge that IOP spikes of this magnitude do not occur in primary open angle glaucoma and its presence might confound our interpretation. Another important limitation of this model is that the mechanism of sustained IOP elevation is not known. If compression alone were the cause then one would expect IOP to return to normal even with the suture in place, simply due to acclimatisation of the eye. A likely alternative is that there is compression of vessels, and thus increased venous pressure that could reduce aqueous outflow. We have previously ruled out the possibility that vessel

This article is protected by copyright. All rights reserved

Author Manuscript

compression affects the retinal blood flow producing non-IOP related vascular compromise.[10]

In conclusion, these preliminary findings suggest that ganglion cell dysfunction induced by eight weeks of mild IOP elevation using a circumlimbal suture in rodents is reversible with IOP lowering via suture removal. With further validation the circumlimbal suture model could provide a platform for investigating the reversibility of neural degeneration from chronic IOP challenge.

Acknowledgements: Dr Jelena Kezic and Dr Xiangting Chen from Monash University assisted with the slide scanning for the histological assessment. This study was supported by National Health and Medical Research Council of Australia grants (1046203) and an Australian Research Council Fellowship (FT130100388). The funding bodies had no involvement in study design; in the collection, analysis and interpretation of data; in the writing of the report; and in the decision to submit the article for publication. Author contributions are: Conceived and designed the experiments: HHL, ZH, CTN, BVB, AJV. Performed the experiments: HHL, ZH, CTN, BVB. Analyzed the data: HHL, ZH, CTN, BVB, AJV. Wrote the paper: HHL, ZH, CTN, BVB, AJV.

Disclosures: The authors report no conflicts of interest and have no proprietary interest in any of the materials mentioned in this article.

References

1. Banitt MR, *et al.* (2013) Progressive loss of retinal ganglion cell function precedes structural loss by several years in glaucoma suspects. *Invest Ophthalmol Vis Sci*;54:2346-2352.

2. Porciatti V & Nagaraju M (2010) Head-up tilt lowers IOP and improves RGC dysfunction in glaucomatous DBA/2J mice. *Exp Eye Res*;90:452-460.

3. He Z, Bui BV & Vingrys AJ (2008) Effect of repeated IOP challenge on rat retinal function. *Invest Ophthalmol Vis Sci*;49:3026-3034.

4. Ventura LM & Porciatti V (2005) Restoration of retinal ganglion cell function in early glaucoma after intraocular pressure reduction: a pilot study. *Ophthalmology*;112:20-27.

5. Sehi M, Grewal DS, Goodkin ML & Greenfield DS (2010) Reversal of retinal ganglion cell dysfunction after surgical reduction of intraocular pressure. *Ophthalmology*;117:2329-2336.

This article is protected by copyright. All rights reserved

Author Manuscript

6. Ventura LM, Feuer WJ & Porciatti V (2012) Progressive loss of retinal ganglion cell function is hindered with IOP-lowering treatment in early glaucoma. *Invest Ophthalmol Vis Sci*;53:659-663.

7. Niyadurupola N, *et al*. (2013) Intraocular pressure lowering is associated with an increase in the photopic negative response (PhNR) amplitude in glaucoma and ocular hypertensive eyes. *Invest Ophthalmol Vis Sci*;54:1913-1919.

8. Wright TM, Goharian I, Gardiner SK, Sehi M & Greenfield DS (2015) Short-term enhancement of visual field sensitivity in glaucomatous eyes following surgical intraocular pressure reduction. *Am J Ophthalmol*;159:378-385 e371.

9. Sehi M, Grewal DS, Feuer WJ & Greenfield DS (2011) The impact of intraocular pressure reduction on retinal ganglion cell function measured using pattern electroretinogram in eyes receiving latanoprost 0.005% versus placebo. *Vision Res*;51:235-242.

10. Liu HH, *et al.* (2015) Chronic ocular hypertension induced by circumlimbal suture in rats. *Invest Ophthalmol Vis Sci*;56:2811-2820.

11. Fortune B, Cull G, Reynaud J, Wang L & Burgoyne CF (2015) Relating Retinal Ganglion Cell Function and Retinal Nerve Fiber Layer (RNFL) Retardance to Progressive Loss of RNFL Thickness and Optic Nerve Axons in Experimental Glaucoma. *Invest Ophthalmol Vis Sci*;56:3936-3944.

12. Fortune B, Wang L, Cull G & Cioffi GA (2008) Intravitreal colchicine causes decreased RNFL birefringence without altering RNFL thickness. *Invest Ophthalmol Vis Sci*;49:255-261.

13. Weber AJ & Harman CD (2005) Structure-function relations of parasol cells in the normal and glaucomatous primate retina. *Invest Ophthalmol Vis Sci*;46:3197-3207.

14. Leung CK, *et al.* (2011) Long-term in vivo imaging and measurement of dendritic shrinkage of retinal ganglion cells. *Invest Ophthalmol Vis Sci*;52:1539-1547.

15. Morquette B, *et al*. (2015) REDD2-mediated inhibition of mTOR promotes dendrite retraction induced by axonal injury. *Cell Death Differ*;22:612-625.

16. Weitlauf C, *et al.* (2014) Short-term increases in transient receptor potential vanilloid-1 mediate stress-induced enhancement of neuronal excitation. *J Neurosci*;34:15369-15381.

17. Weymouth AE & Vingrys AJ (2008) Rodent electroretinography: methods for extraction and interpretation of rod and cone responses. *Prog Retin Eye Res*;27:1-44.

18. Bui BV, Edmunds B, Cioffi GA & Fortune B (2005) The Gradient of Retinal Functional Changes during Acute Intraocular Pressure Elevation. *Invest Ophthalmol Vis Sci*;46:202-213.

19. Bui BV & Fortune B (2004) Ganglion cell contributions to the rat full-field electroretinogram. *J Physiol*;555:153-173.

20. Hood DC & Birch DG (1994) Rod phototransduction in retinitis pigmentosa: estimation and interpretation of parameters derived from the rod a-wave. *Invest Ophthalmol Vis Sci*;35:2948-2961.

This article is protected by copyright. All rights reserved

Author Manuscript

21. Lamb TD & Pugh EN, Jr. (1992) A quantitative account of the activation steps involved in phototransduction in amphibian photoreceptors. *J Physiol*;449:719-758.

22. Fulton AB & Rushton WA (1978) The human rod ERG: correlation with psychophysical responses in light and dark adaptation. *Vision Res*;18:793-800.

23. McGilchrist CA (1993) REML estimation for survival models with frailty. *Biometrics*;49:221-225.

24. Cnaan A, Laird NM & Slasor P (1997) Using the general linear mixed model to analyse unbalanced repeated measures and longitudinal data. *Stat Med*;16:2349-2380.

25. Caprioli J, *et al*. (2016) Trabeculectomy Can Improve Long-Term Visual Function in Glaucoma. *Ophthalmology*;123:117-128.

26. Waisbourd M, *et al.* (2016) Reversible structural and functional changes after intraocular pressure reduction in patients with glaucoma. *Graefes Arch Clin Exp Ophthalmol*;

27. Ventura LM, *et al.* (2011) Head-down Posture Induces PERG Alterations in Early Glaucoma. *J Glaucoma*;22:255-264.

28. Porciatti V & Nagaraju M (2010) Head-up tilt lowers IOP and improves RGC dysfunction in glaucomatous DBA/2J mice. *Exp Eye Res*;90:452-460.

29. He Z, Bui BV & Vingrys AJ (2006) The rate of functional recovery from acute IOP elevation. *Invest Ophthalmol Vis Sci*;47:4872-4880.

30. Nagaraju M, Saleh M & Porciatti V (2007) IOP-dependent retinal ganglion cell dysfunction in glaucomatous DBA/2J mice. *Invest Ophthalmol Vis Sci*;48:4573-4579.

31. Nguyen CT, Vingrys AJ, Wong VH & Bui BV (2013) Identifying cell class specific losses from serially generated electroretinogram components. *Biomed Res Int*;2013:796362.

32. Della Santina L, Inman DM, Lupien CB, Horner PJ & Wong RO (2013) Differential progression of structural and functional alterations in distinct retinal ganglion cell types in a mouse model of glaucoma. *J Neurosci*;33:17444-17457.

33. Weber AJ, Kaufman PL & Hubbard WC (1998) Morphology of single ganglion cells in the glaucomatous primate retina. *Invest Ophthalmol Vis Sci*;39:2304-2320.

34. Shou T, Liu J, Wang W, Zhou Y & Zhao K (2003) Differential dendritic shrinkage of alpha and beta retinal ganglion cells in cats with chronic glaucoma. *Invest Ophthalmol Vis Sci*;44:3005-3010.

35. Morgan JE, Datta AV, Erichsen JT, Albon J & Boulton ME (2006) Retinal ganglion cell remodelling in experimental glaucoma. *Adv Exp Med Biol*;572:397-402.

36. Li L, *et al*. (2008) Protective role of reactive astrocytes in brain ischemia. *J Cereb Blood Flow Metab*;28:468-481.

37. Burda JE, Bernstein AM & Sofroniew MV (2016) Astrocyte roles in traumatic brain injury. *Exp Neurol*;275 Pt 3:305-315.

This article is protected by copyright. All rights reserved

Author Manuscript

38. Abbott CJ, *et al.* (2014) Evaluation of retinal nerve fiber layer thickness and axonal transport 1 and 2 weeks after 8 hours of acute intraocular pressure elevation in rats. *Invest Ophthalmol Vis Sci*;55:674-687.

39. Chidlow G, Wood JP, Ebneter A & Casson RJ (2012) Interleukin-6 is an efficacious marker of axonal transport disruption during experimental glaucoma and stimulates neuritogenesis in cultured retinal ganglion cells. *Neurobiol Dis*;48:568-581.

40. Kloda A, Lua L, Hall R, Adams DJ & Martinac B (2007) Liposome reconstitution and modulation of recombinant N-methyl-D-aspartate receptor channels by membrane stretch. *Proc Natl Acad Sci U S A*;104:1540-1545.

41. Tezel G (2009) The role of glia, mitochondria, and the immune system in glaucoma. *Invest Ophthalmol Vis Sci*;50:1001-1012.

42. Dong CJ, Guo Y, Agey P, Wheeler L & Hare WA (2008) Alpha2 adrenergic modulation of NMDA receptor function as a major mechanism of RGC protection in experimental glaucoma and retinal excitotoxicity. *Invest Ophthalmol Vis Sci*;49:4515-4522.

43. Seitz R, Ohlmann A & Tamm ER (2013) The role of Muller glia and microglia in glaucoma. *Cell Tissue Res*;353:339-345.

44. Wheeler-Schilling TH, Marquordt K, Kohler K, Guenther E & Jabs R (2001) Identification of purinergic receptors in retinal ganglion cells. *Brain Res Mol Brain Res*;92:177-180.

45. Ryskamp DA, *et al.* (2011) The polymodal ion channel transient receptor potential vanilloid 4 modulates calcium flux, spiking rate, and apoptosis of mouse retinal ganglion cells. *J Neurosci*;31:7089-7101.

46. Crish SD & Calkins DJ (2011) Neurodegeneration in glaucoma: progression and calcium-dependent intracellular mechanisms. *Neuroscience*;176:1-11.

47. Domenici L, *et al.* (2014) Rescue of retinal function by BDNF in a mouse model of glaucoma. *PLoS One*;9:e115579.

48. Valiente-Soriano FJ, *et al*. (2015) BDNF Rescues RGCs But Not Intrinsically Photosensitive RGCs in Ocular Hypertensive Albino Rat Retinas. *Invest Ophthalmol Vis Sci*;56:1924-1936.

49. Sappington RM, *et al.* (2015) Activation of transient receptor potential vanilloid-1 (TRPV1) influences how retinal ganglion cell neurons respond to pressure-related stress. *Channels (Austin)*;9:102-113.

50. Kong YX, *et al.* (2012) Impact of aging and diet restriction on retinal function during and after acute intraocular pressure injury. *Neurobiol Aging*;33:1126 e1115-1125.

51. Tang SH, Yu JG, Li JJ & Sun JY (2015) Neuroprotective effect of ketamine on acute spinal cord injury in rats. *Genet Mol Res*;14:3551-3556.

This article is protected by copyright. All rights reserved

Author Manuscript

52. Chauhan BC, *et al*. (2002) Effect of intraocular pressure on optic disc topography, electroretinography, and axonal loss in a chronic pressure-induced rat model of optic nerve damage. *Invest Ophthalmol Vis Sci*;43:2969-2976.

53. Danias J, *et al.* (2006) Characterization of retinal damage in the episcleral vein cauterization rat glaucoma model. *Exp Eye Res*;82:219-228.

54. Grozdanic SD, Kwon YH, Sakaguchi DS, Kardon RH & Sonea IM (2004) Functional evaluation of retina and optic nerve in the rat model of chronic ocular hypertension. *Exp Eye Res*;79:75-83.

Author Manuscript

FIGURE CAPTIONS

Figure 1. Reversing chronic intraocular pressure (IOP) elevation in the rat circumlimbal suture model. After an initial IOP spike during suture application, chronic IOP elevation was maintained for the next 8 weeks (n = 7, red symbols). IOP dropped (green symbols) to levels comparable to fellow control eyes (n = 7, black symbols) after removal of the suture (green reference line). Baseline for the treated eyes shown in grey.

Figure 2. Effect of chronic intraocular pressure (IOP) elevation, followed by IOP lowering on retinal function. **A.** Averaged ERG responses at baseline (week 0) from the dimmest (lowest) to the brightest (upper most) from contralateral control (n = 7, black traces) and treated eyes (red traces). **B.** Averaged electroretinogram (ERG) waveforms at week 8 prior to IOP lowering **C.** Averaged ERG waveforms in control (black traces) and treated eyes after IOP lowering (green traces).

Figure 3. Outer and inner retinal deficits during intraocular pressure (IOP) elevation and following IOP lowering. **A**. Averaged electroretinogram (ERG) responses for the brightest luminous energy (2.07 log cd.s.m^{-2}) for contralateral control (n = 7, black trace) and treated eyes (n = 7, coloured trace) at each time point compared with the 96% confidence limits measured at baseline (grey area). During IOP elevation responses were attenuated (red traces), but recovered with IOP lowering (green traces). **B.** As per **A** but waveforms show the scotopic threshold response measured at -5.01 log cd.s.m^{-2}.

This article is protected by copyright. All rights reserved

Figure 4. Comparison of photoreceptor, bipolar cell and ganglion cell function with intraocular pressure (IOP) elevation and lowering. **A.** Average (± standard error of the mean) amplitude for contralateral control (n = 7, filled) compared with treated eyes (n = 7) during (red) IOP elevation and after IOP lowering (green). **B.** Control (unfilled) and treated eyes (IOP elevation, red: IOP lowering, green) expressed as a percentage of baseline. **C.** and **D.** are as per A and B, respectively except that they show b-wave amplitude as a function of time. **E.** and **F.** are as per A and B, respectively, except that they show positive Scotopic Threshold Response (pSTR) amplitude.

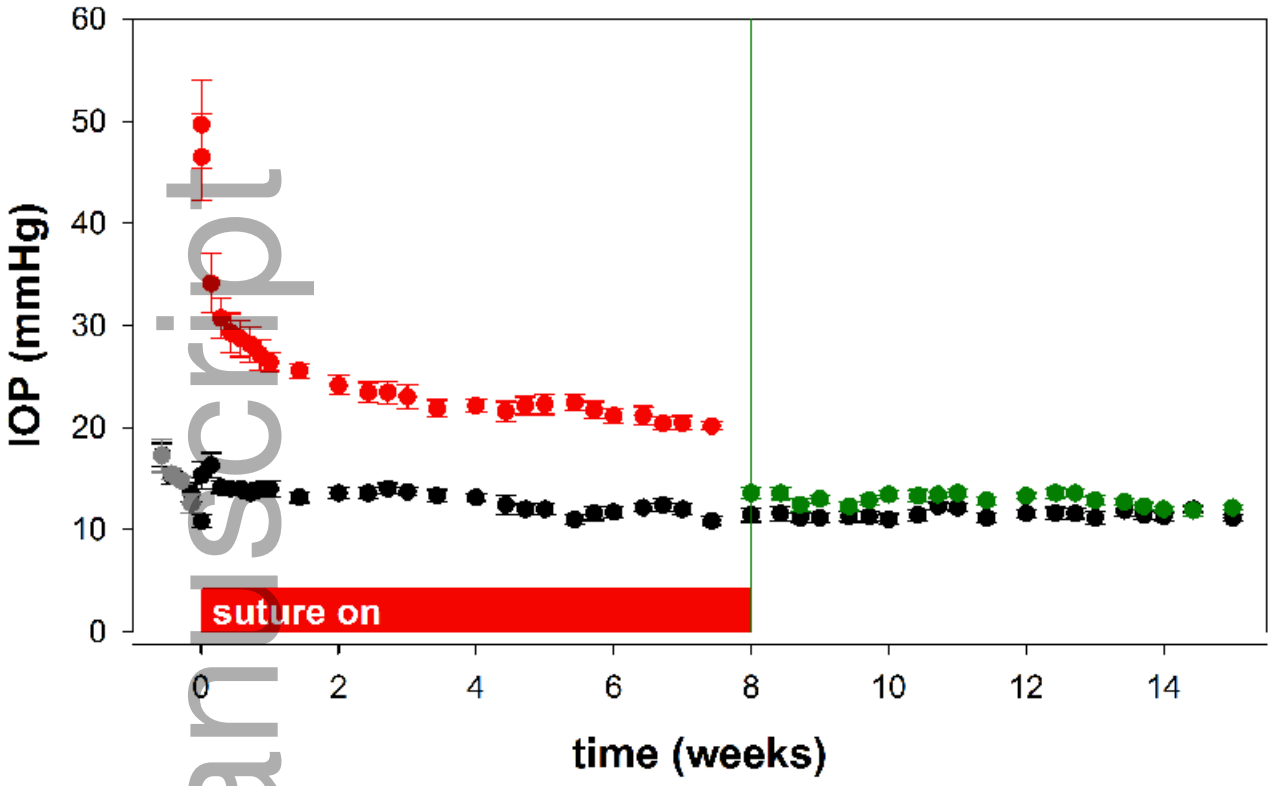
Figure 5. Effect of intraocular pressure (IOP) elevation and lowering on retinal and retinal nerve fiber layer (RNFL) thickness measured using spectral domain optical coherence tomography. **A.** Average (± standard error of the mean) total retinal thickness for contralateral control (n = 7, filled) compared with treated eyes (n = 7) during (red) IOP elevation and after IOP lowering (green). **B.** Thicknesses for control (unfilled) and treated eyes (IOP elevation, red: IOP lowering, green) expressed as a percentage of baseline. **C.** and **D.** are as per A and B, respectively, except that they show RNFL thickness as a function of time.

Figure 6. Retinal histology at week 15. **A.** Representative contralateral control and **B.** treated eyes stained with hematoxylin and eosin stain. **C.** Average cell density (± standard error of the mean) in the ganglion cell layer (GCL) of control (black bar, n = 7) and treated eyes (green bar, n = 7). Scale bar: 100 µm.

Figure 7. Correlations between cell density, optical coherence tomography (OCT) and electroretinogram (ERG) parameters after intraocular pressure (IOP) lowering. **A.** Relationship between photoreceptoral amplitude and cell density for control (black symbols, n = 7) and treated eyes (green symbols, n = 7). **B.** Relationship between the positive Scotopic Threshold Response (pSTR) and cell density. Linear regressions are plotted along with the 95% confidence limit around the slopes of the function. **C.** Relationship between retinal nerve fiber layer (RNFL) thickness and cell density. **D.** Relationship between pSTR and RNFL thickness.

Author Manuscript

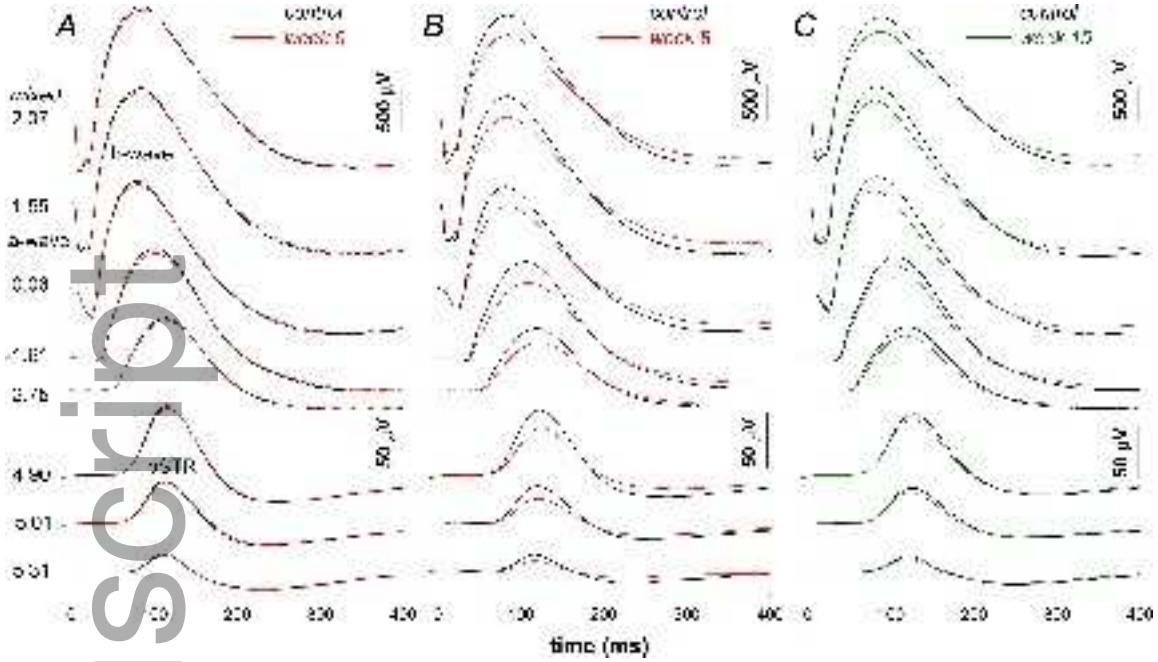
This article is protected by copyright. All rights reserved



opo_12331_f1.jpg

Author Manuscript

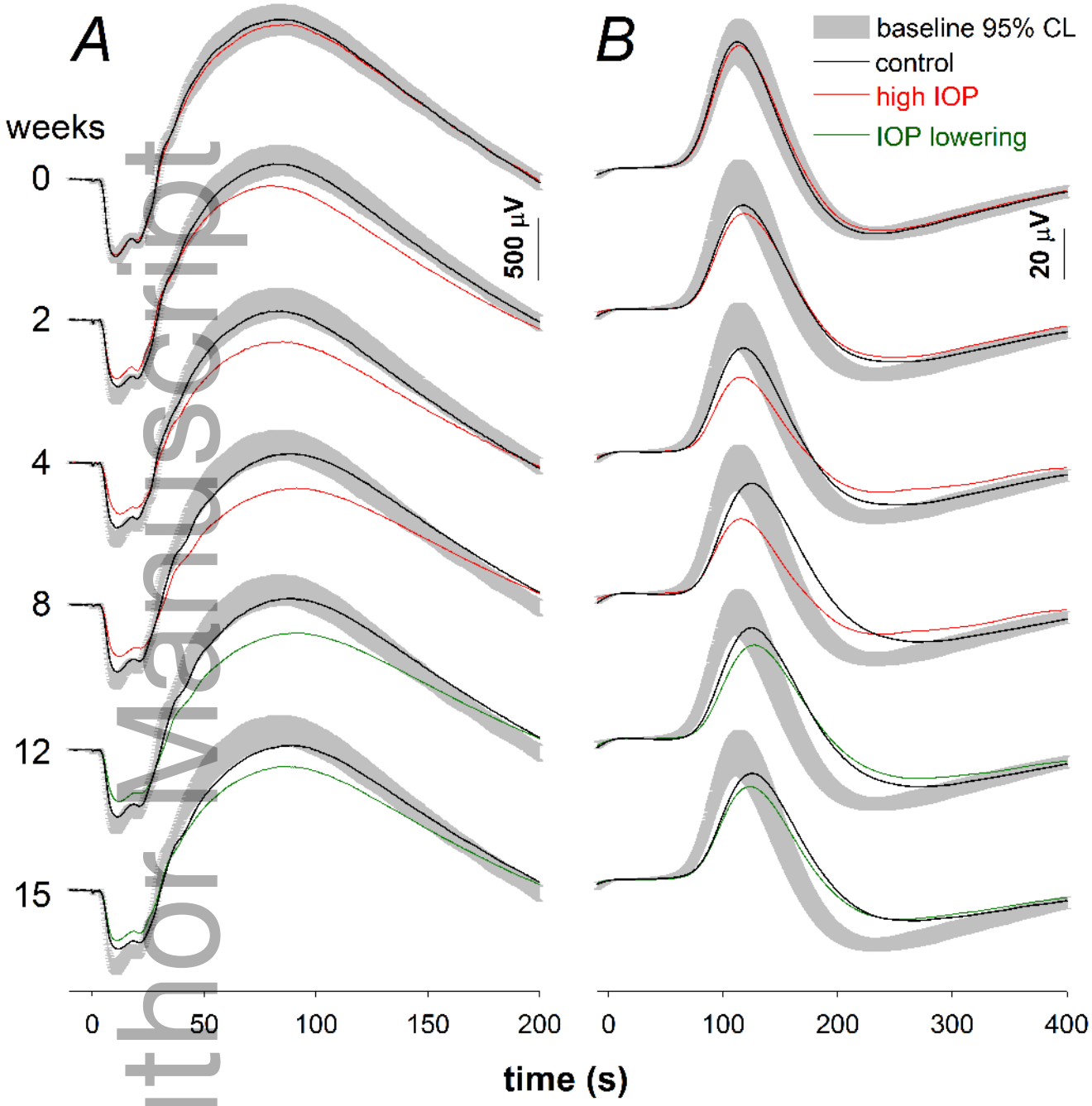
This article is protected by copyright. All rights reserved



opo_12331_f2.jpg

Author Manuscript

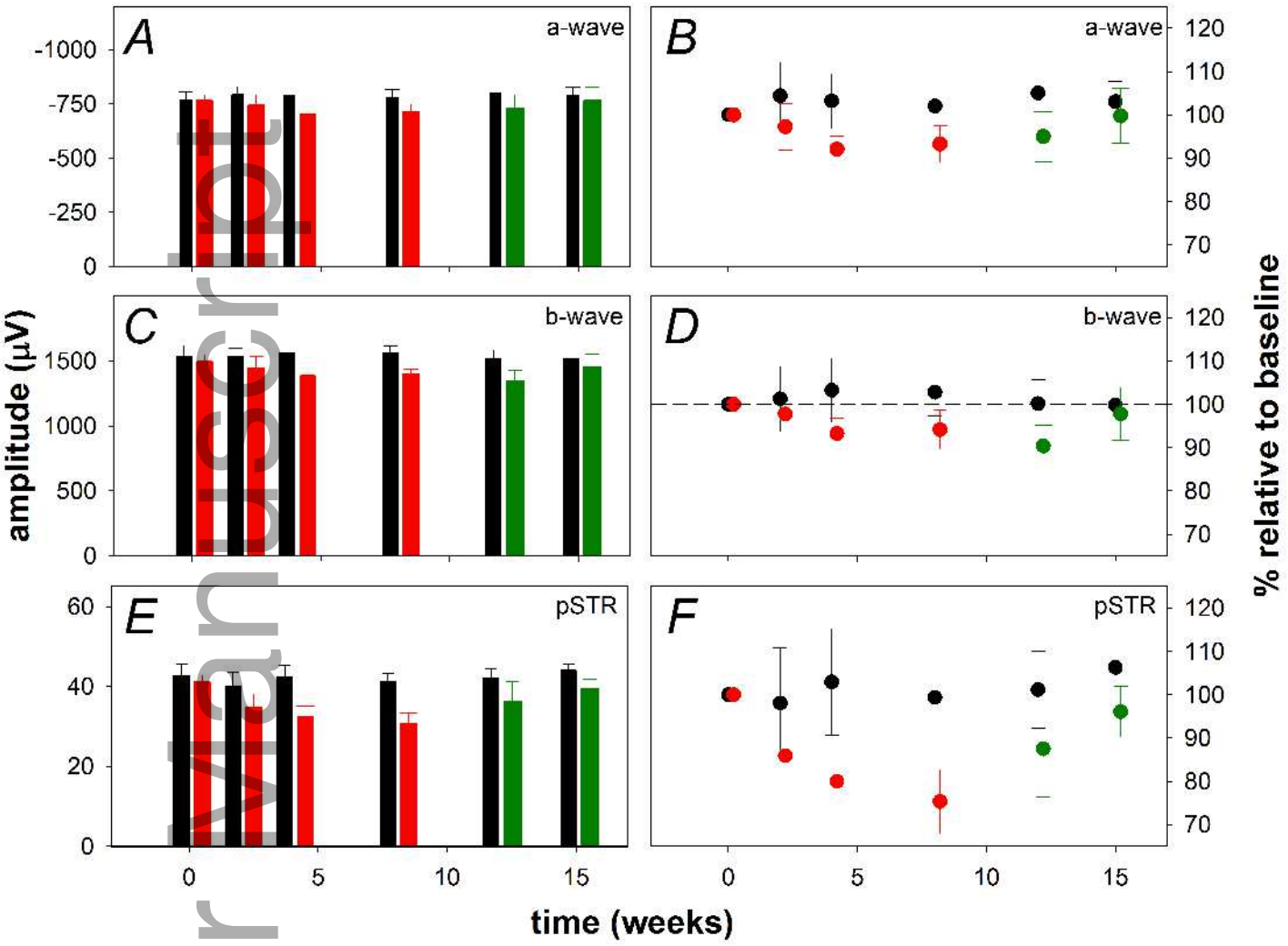
This article is protected by copyright. All rights reserved



opo_12331_f3.jpg

Author Manuscript

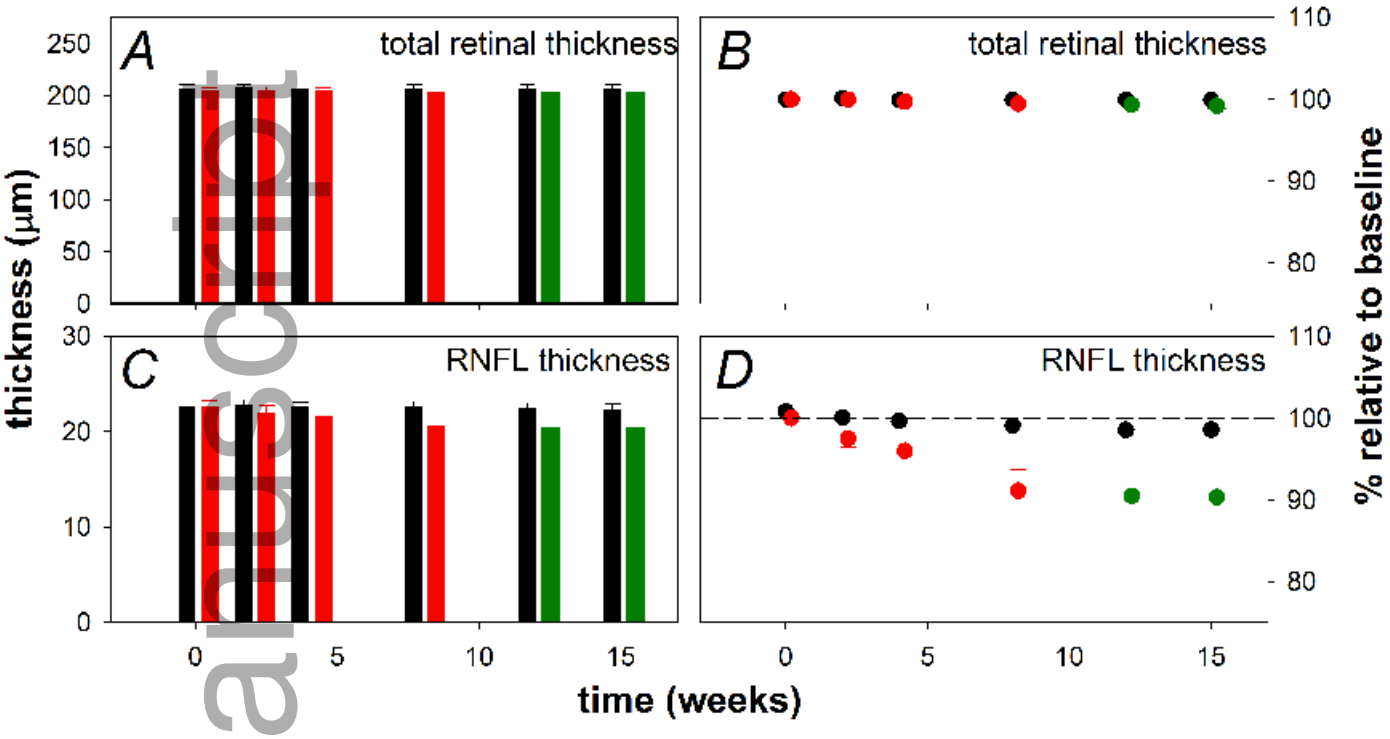
This article is protected by copyright. All rights reserved



opo_12331_f4.jpg

Author Manuscript

This article is protected by copyright. All rights reserved

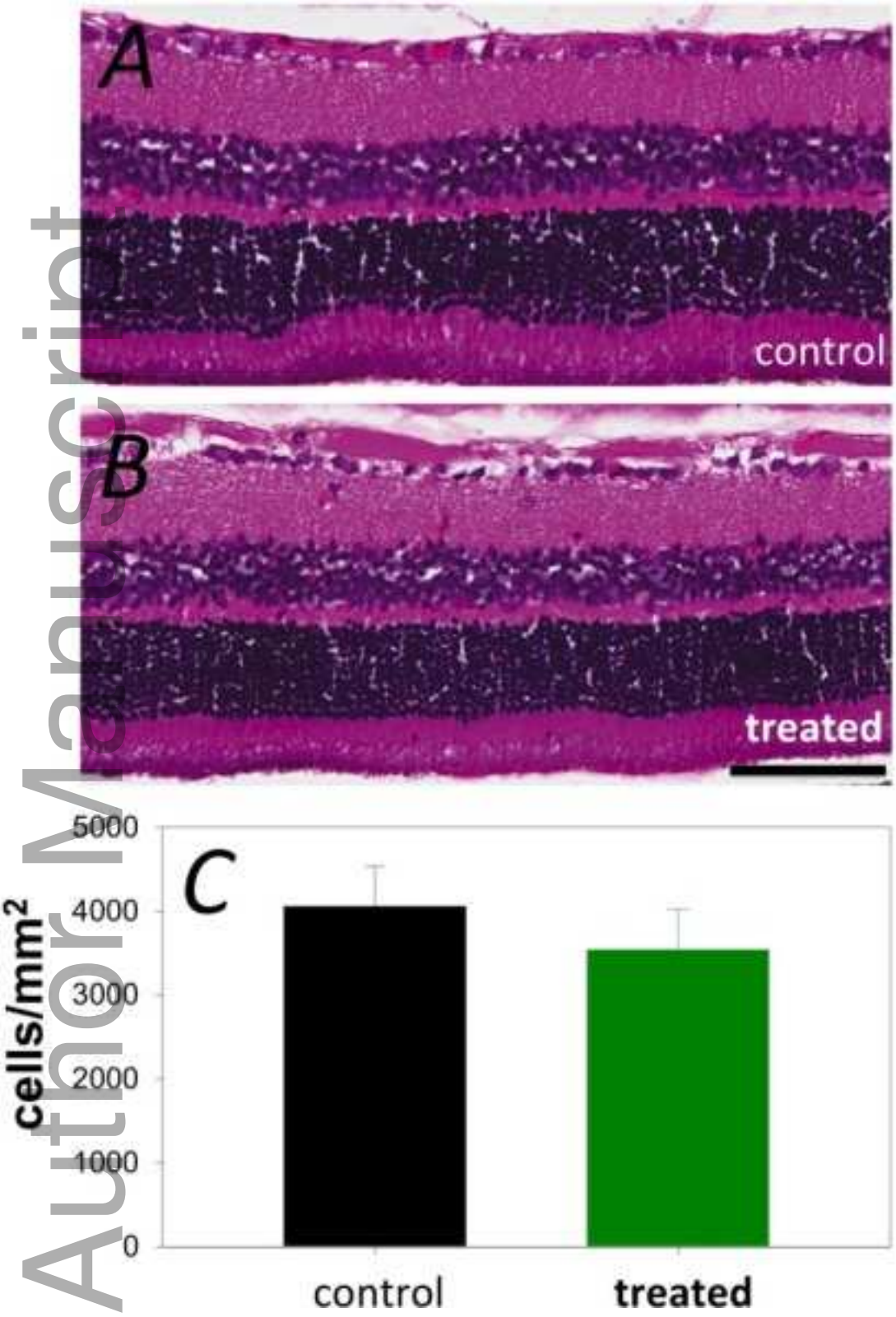


opo_12331_f5.jpg

Author Manuscript

This article is protected by copyright. All rights reserved

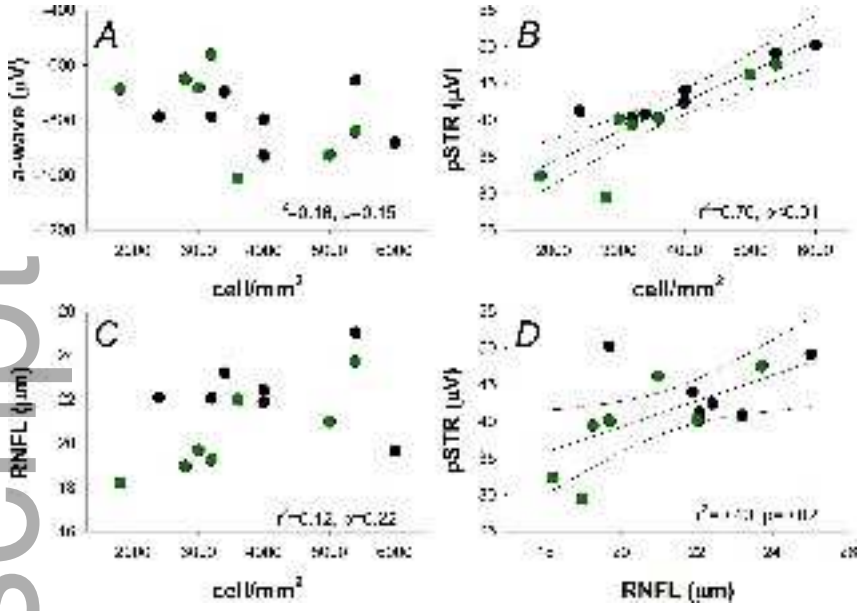
Author Manuscript



opo_12331_f6.jpg

This article is protected by copyright. All rights reserved

Author Manuscript



opo_12331_f7.jpg

This article is protected by copyright. All rights reserved